A Simplified Braking Method for Direct Matrix Converter-Fed PMSM Drives with Consideration of Avoiding Regenerative Energy

Jun Xie, Dustin Henneberg, Martin Suberski, Thomas Ellinger,
Uwe Rädel and Jürgen Petzoldt
Technische Universität Ilmenau
Power Electronics and Control Group
Ilmenau, Germany
Phone: +49 367769-1553
Fax: +49 367769-1469
Email: jun.xie@tu-ilmenau.de
URL: http://www.tu-ilmenau.de

Keywords

≪Direct matrix converter≫, ≪AC-AC converter≫, ≪Permanent magnet motor≫, ≪Variable speed drive≫, ≪Regenerative power≫

Abstract

This paper presents a simplified braking method for direct matrix converter (DMC) - fed permanent magnet synchronous motor (PMSM) drives with special consideration of avoiding the regenerative energy from feeding back to the grid. As a four-quadrant converter, the DMC has the bidirectional energy-flow capability, which is seen as a great benefit. However, the regenerative energy feeding back to the grid is not always needed, in some cases might be not allowed or not possible. These could happen due to the grid load status, strict quality specifications of the grid current or grid failure, where the DMC needs to be decoupled from the grid. In order to avoid the regenerative energy temporarily or completely, a three-phase diode bridge (B6) with chopper resistance on the motor side is employed together with the traditional B12-clamp circuit, which is used for overvoltage protection. Furthermore, the motor torque during braking could be controlled without large fluctuation and within the required limitation. The principle of the proposed strategy is described in detail. Simulation results are used to verify the feasibility of the proposed strategy.

Introduction

The three-phase DMC shown in Fig. 1 currently attracts many research interests in power electronics and power systems [1, 2]. As an alternative topology of direct AC-AC conversion without any bulky energy storage elements in an intermediate link, the DMC shows great advantages with its compact size, bidirectional energy-flow capability and longtime durability, especially in adjustable speed drives applications.

Compared with the conventional AC-DC-AC converter, which also has the bidirectional energy-flow capability as shown in Fig. 2 (a), the DMC has no energy storage components in the DC-link, which is a great benefit in volume, since no additional circuit is required. However, the harmonics involved in the grid current could be an issue for DMC in applications, where strict quality specifications are required.

On the other hand, the regenerative energy could be temporarily undesired according to the grid load status, especially for micro grid with many loads in parallel, where the power flow in the grid must be controlled properly to keep the grid stable. It could also happen, when there is error in grid and the

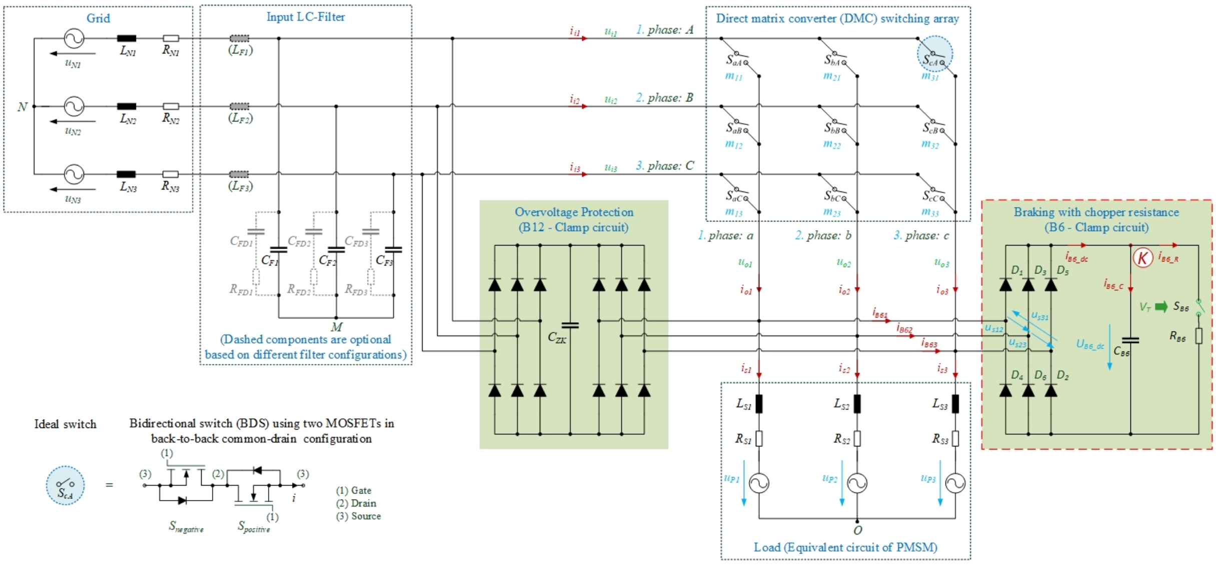

Fig. 1: System topology of three-phase to three-phase DMC-fed PMSM drives with braking circuit for avoiding regenerative energy

DMC needs to be decoupled from the grid, in this case, the regenerative energy is not able to feed back to the grid. For these reasons, it is important to have a control method to avoid the regenerative energy temporarily or completely. So far, not much researches are made in this potential application and more research interests are expected in this field.

In [6–8], continue studies for avoiding regenerative energy are presented with three different methods in the special application of electric aircraft, which is a great foundation for further study. In [6], B6-diode bridge with one chopper resistance on the grid side is as input power clamp (IPC) method employed as shown in Fig. 2 (b). In [7], three-phase chopper resistance on the grid side is implemented as bi-directional switch (BDS) method as shown in Fig. 2 (c). Both methods rely on the detection of regenerative energy. There are two methods presented for detecting regenerative energy. The first method is the power comparison (PC) method, in which the input and output power are estimated separately and the result of comparison is then used as reference for duty cycle calculation of the related chopper switches. The second method is the input voltage reference (IVR) method, in which the input capacitor voltage is used as reference. In [8], the standard B12-clamp circuit is used with a chopper resistance in the DC-link as shown in Fig. 2 (d). In [9], further studies are made with special consideration of gird faults in regeneration in order to properly decide the halt sequence of the DMC.

In conclusion, all these methods above show good results and have specific advantages and some shortcomings to some extent. This paper proposed a simplified method for braking of DMC-fed PMSM drives with consideration of avoiding regenerative energy. As shown in Fig. 1, in normal drive operation, the chopper resistance R_{B6} in the B6-diode bridge is shut down by chopper switch S_{B6}. When the PMSM drive brakes, the switching matrix of DMC is shut down by disabling the gate signals and the chopper switch S_{B6} starts to switching according to the duty cycle V_t, which is determined by the proposed control strategy. The energy stored in PMSM drives will be consumed by the chopper resistance R_{B6} to avoid the regenerative energy back to the grid. Meanwhile, the braking moment *mi* in this period could be controlled within the required limitation as long as the duty cycle V_t of the chopper switch S_{B6} still inner the upper limit of 1.

Compared with previous research, the main features of the proposed strategy are as follows:

- It provides a simplified braking method by employing B6-diode bridge with one chopper resistance on motor side and shutting down the switching matrix of DMC during regeneration. The DC-link current in B6-diode bridge $i_{B6,dc}$ is used as reference without calculating power on both sides of DMC, which needs less computation effort.

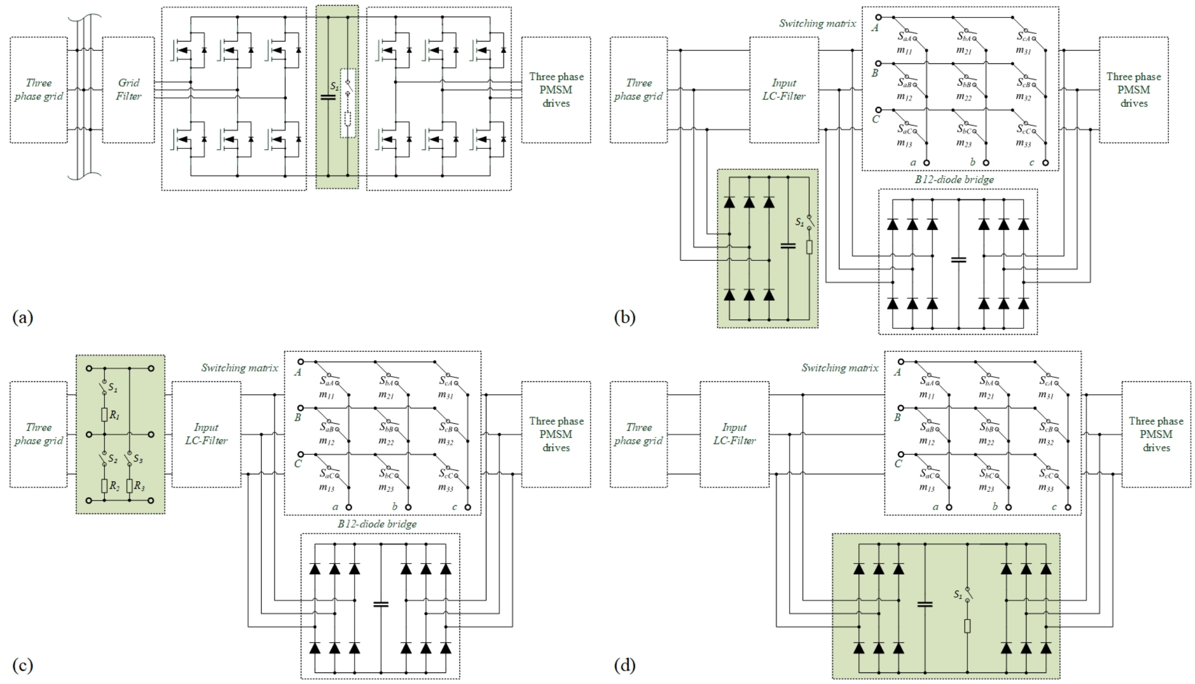

Fig. 2: Summary of methods for avoiding regenerative energy: (a) Conventional AC-DC-AC converter. (b) B6-diode bridge with one chopper resistance on grid side. (c) Three-phase chopper resistance on grid side. (d) Standard B12-clamp circuit with chopper resistance.

- It prevents grid failure to further reflect to the motor drive side though the coupled switching matrix of DMC and keeps the harmonics, which are generated through the B6-diode bridge, away from the grid.
- It is able to control the motor torque within the required limitation and without large fluctuation during braking period, which helps to ensure the motor braking safe and smooth.

The rest of this paper is organized as follows. In section II, a brief introduction of the system topology is presented. The proposed strategy is subsequently addressed in section III. Simulation results verifying the performance of the proposed strategy are demonstrated in section IV. Finally, this study is summarized in section V.

System topology

The system topology of three-phase to three-phase DMC-fed PMSM drives with avoiding regenerative energy is shown in Fig. 1, which consists of power supply, input *LC* filter, DMC switching array, PMSM drive system, the B12-clamp circuit for overvoltage protection and the B6-diode bridge for braking.

A. Topology of DMC

The DMC is composed of nine bidirectional switches (BDS) as a 3×3 matrix, which connects the grid to the PMSM drives. Each BDS should have the capability to block voltage and conduct current in both directions. There are many configurations for the realization [12]. One possibility could be two power semiconductor switches in back-to-back arrangement, which is shown in Fig. 1. The power semiconductor switch used could be anti-parallel insulated gate bipolar transistor (IGBT) or metal–oxide–semiconductor field-effect transistor (MOSFET).

The input *LC*-Filter is necessary to reduce high-frequency current harmonics and voltage fluctuation. Many topologies of input filter for DMC have been proposed [10]. In this study, the damped *LC* filter is employed, in which the filter capacitor C_f is parallel with a *RC* damping circuit as shown in Fig. 1. It is worth noticing that, if the grid impedance $(R_N + jX_{L_N})$ can be precisely determined, it is possible to use grid inductance L_N instead of the normal filter inductance L_f within the permissible resonance frequency range. The output filter is commonly neglected due to the inductive nature of PMSM drive system.

The B12-clamping circuit is frequently implemented as a standard circuit for overvoltage protection, which makes up the deficiencies of DMC for absence of passive free-wheeling paths. It connects the input and output sides of DMC using 12 fast recovery diodes. The double B6 diode bridge are connected by a DC-link capacitor C_{ZK}, which is determined proportional to the energy stored in PMSM drives [11].

The B6-diode bridge is employed to avoid the regenerative energy by motor braking. The chopper resistance R_{B6} is switched at duty cycle V_t, which is determined by the control strategy. The DC-link capacitor of the B6-diode bridge C_{B6} is used for voltage measurement and to absorb the high frequency components of the chopper resistance current $i_{B6,R}$.

B. Direct modulation strategy of DMC

The direct modulation strategy, namely the optimized Venturini's method, is employed for normal operation of the PMSM drives in the study, because of its convenience and straightforward of understanding the basics of DMC.

The switching status S_{ij} of each BDS in the 3×3 switching array can be assigned as 1 to represent ON state and 0 to represent OFF state. In this manner, to avoid short circuit of input phases (A,B,C) or open circuit of output phases (a,b,c), the possible switching states to satisfy the constraint (1) is well known to be $3^3 = 27$ combinations.

$$\sum_{j=A,B,C} S_{ij} = 1,\ \forall i = \{a,b,c\} \tag{1}$$

The mathematical relationship between input and output of DMC can be described in (2) with the 3×3 instantaneous transfer matrix of switching state S_{ij}.

$$\begin{bmatrix} u_{o1} \\ u_{o2} \\ u_{o3} \end{bmatrix} = \begin{bmatrix} S_{aA} & S_{aB} & S_{aC} \\ S_{bA} & S_{bB} & S_{bC} \\ S_{cA} & S_{cB} & S_{cC} \end{bmatrix} \begin{bmatrix} u_{i1} \\ u_{i2} \\ u_{i3} \end{bmatrix} \quad , \quad \begin{bmatrix} i_{i1} \\ i_{i2} \\ i_{i3} \end{bmatrix} = \begin{bmatrix} S_{aA} & S_{aB} & S_{aC} \\ S_{bA} & S_{bB} & S_{bC} \\ S_{cA} & S_{cB} & S_{cC} \end{bmatrix}^T \begin{bmatrix} i_{o1} \\ i_{o2} \\ i_{o3} \end{bmatrix} \tag{2}$$

where $\vec{u}_i = \begin{bmatrix} u_{i1} & u_{i2} & u_{i3} \end{bmatrix}^T$ and $\vec{i}_i = \begin{bmatrix} i_{i1} & i_{i2} & i_{i3} \end{bmatrix}^T$, $\vec{u}_o = \begin{bmatrix} u_{o1} & u_{o2} & u_{o3} \end{bmatrix}^T$ and $\vec{i}_o = \begin{bmatrix} i_{o1} & i_{o2} & i_{o3} \end{bmatrix}^T$ are the input and output voltage and current vectors respectively.

Suppose the sinusoidal input voltage vector $\vec{u}_i$ and output current vector $\vec{i}_o$ of DMC are expressed as (3):

$$\vec{u}_i(t) = \begin{bmatrix} \hat{U}_i cos(\omega_i t) \\ \hat{U}_i cos(\omega_i t - \frac{2\pi}{3}) \\ \hat{U}_i cos(\omega_i t + \frac{2\pi}{3}) \end{bmatrix} \quad , \quad \vec{i}_o(t) = \begin{bmatrix} \hat{I}_o cos(\omega_o t + \phi_o) \\ \hat{I}_o cos(\omega_o t - \frac{2\pi}{3} + \phi_o) \\ \hat{I}_o cos(\omega_o t + \frac{2\pi}{3} + \phi_o) \end{bmatrix} \tag{3}$$

By adding third harmonics of the input and output angular frequencies into the desired output voltage, a maximum voltage transfer ratio q of $\frac{\sqrt{3}}{2}$ (or 86.7%) is achieved, which is known as the intrinsic limitation of DMC [12]. The desired output voltage vector $\vec{u}_o$ and input current vector $\vec{i}_i$ in average value are described as (4).

$$\vec{u}_o(t) = q\hat{U}_i \begin{bmatrix} cos(\omega_o t) - \frac{1}{6}cos(3\omega_o t) + \frac{1}{2\sqrt{3}}cos(3\omega_i t) \\ cos(\omega_o t - \frac{2\pi}{3}) - \frac{1}{6}cos(3\omega_o t) + \frac{1}{2\sqrt{3}}cos(3\omega_i t) \\ cos(\omega_o t + \frac{2\pi}{3}) - \frac{1}{6}cos(3\omega_o t) + \frac{1}{2\sqrt{3}}cos(3\omega_i t) \end{bmatrix} \ , \ \vec{i}_i(t) = \begin{bmatrix} \hat{I}_i cos(\omega_i t + \phi_i) \\ \hat{I}_i cos(\omega_i t - \frac{2\pi}{3} + \phi_i) \\ \hat{I}_i cos(\omega_i t + \frac{2\pi}{3} + \phi_i) \end{bmatrix} \tag{4}$$

where f_i and f_o are the input and output frequencies with $\omega_i = 2\pi f_i$ and $\omega_o = 2\pi f_o$; q is the voltage transfer ratio with $q = \frac{\hat{U}_o}{\hat{U}_i}$; $\hat{U}_i$ and $\hat{U}_o$, $\hat{I}_i$ and $\hat{I}_o$ are the input and output voltage and current amplitude, respectively; ϕ_i and ϕ_o are the input and output phase displacement angle.

By employing unity input power factor with $cos(\phi_i) = 1$ into the direct modulation method, the duty cycle $m_{ij}(t)$ of each switch is expressed in a simplified form in (5).

$$\begin{aligned} m_{ij}(t) =& \frac{1}{3}\left\{1+2q\cdot cos\left(\omega_i t-(j-1)\frac{2\pi}{3}\right)\left[cos\left(\omega_o t-(i-1)\frac{2\pi}{3}\right)-\frac{1}{6}cos(3\omega_o t)\right]\right. \\ &\left.+\frac{7}{12}cos\left(2\omega_i t+(j-1)\frac{2\pi}{3}\right)-\frac{1}{12}cos\left(4\omega_i t-(j-1)\frac{2\pi}{3}\right)\right\} \end{aligned} \tag{5}$$

where $\forall i=\{1,2,3\}$ corresponds to output phase $\{a,b,c\}$ and $\forall j=\{1,2,3\}$ corresponds to input phase $\{A,B,C\}$. With $\vartheta_i=\omega_i t$ and $\vartheta_o=\omega_o t$, the entire transfer matrix can be expressed using duty cycles $m_{ij}(t)$ with the vectors defined in (6) and (7) as shown in (8).

$$\begin{bmatrix}x_1\\x_2\\x_3\end{bmatrix}=\begin{bmatrix}cos(\vartheta_o)-\frac{1}{6}cos(3\vartheta_o)\\cos(\vartheta_o-\frac{2\pi}{3})-\frac{1}{6}cos(3\vartheta_o)\\cos(\vartheta_o+\frac{2\pi}{3})-\frac{1}{6}cos(3\vartheta_o)\end{bmatrix} \quad , \quad \begin{bmatrix}y_1\\y_2\\y_3\end{bmatrix}=\begin{bmatrix}cos(\vartheta_i)\\cos(\vartheta_i-\frac{2\pi}{3})\\cos(\vartheta_i+\frac{2\pi}{3})\end{bmatrix} \tag{6}$$

$$\begin{bmatrix}z_1\\z_2\\z_3\end{bmatrix}=\frac{7}{36}\begin{bmatrix}cos(2\vartheta_i)\\cos\left(2(\vartheta_i-\frac{2\pi}{3})\right)\\cos\left(2(\vartheta_i+\frac{2\pi}{3})\right)\end{bmatrix}-\frac{1}{36}\begin{bmatrix}cos(4\vartheta_i)\\cos\left(4(\vartheta_i-\frac{2\pi}{3})\right)\\cos\left(4(\vartheta_i+\frac{2\pi}{3})\right)\end{bmatrix} \tag{7}$$

$$\begin{bmatrix}m_{11}&m_{12}&m_{13}\\m_{21}&m_{22}&m_{23}\\m_{31}&m_{32}&m_{33}\end{bmatrix}=\begin{bmatrix}\frac{1}{3}+\frac{m}{\sqrt{3}}(x_1y_1+z_1)&\frac{1}{3}+\frac{m}{\sqrt{3}}(x_1y_2+z_2)&\frac{1}{3}+\frac{m}{\sqrt{3}}(x_1y_3+z_3)\\\frac{1}{3}+\frac{m}{\sqrt{3}}(x_2y_1+z_1)&\frac{1}{3}+\frac{m}{\sqrt{3}}(x_2y_2+z_2)&\frac{1}{3}+\frac{m}{\sqrt{3}}(x_2y_3+z_3)\\\frac{1}{3}+\frac{m}{\sqrt{3}}(x_3y_1+z_1)&\frac{1}{3}+\frac{m}{\sqrt{3}}(x_3y_2+z_2)&\frac{1}{3}+\frac{m}{\sqrt{3}}(x_3y_3+z_3)\end{bmatrix} \tag{8}$$

where $m=\frac{q}{\sqrt{3}/2}$ is the modulation index with a range from 0 to 1.

C. Model of PMSM drive system

Since no output filter is required, the motor voltages and currents are actually the output voltages $\vec{u}_o$ and currents $\vec{i}_o$ of DMC. The continuous-time model of the PMSM is given in dq-coordinate in (9):

$$\begin{cases}u_d=R_s i_d-\omega_e\cdot\psi_q+\frac{d\psi_d}{dt}\\u_q=R_s i_q+\omega_e\cdot\psi_d+\frac{d\psi_q}{dt}\end{cases} \quad , \quad \begin{cases}\psi_d=L_d i_d+\psi_m\\\psi_q=L_q i_q\end{cases} \tag{9}$$

The electromagnetic torque m_i and mechanical dynamics of PMSM can be estimated in (10):

$$m_i=\frac{3}{2}P_p(\psi_d i_q-\psi_q i_d) \quad , \quad m_i-m_l-m_r=\frac{1}{J}\frac{d\omega_m}{dt} \quad , \quad m_r=k_r\omega_m \quad , \quad \omega_e=P_p\cdot\omega_m \tag{10}$$

where u_d and u_q, i_d and i_q, ψ_d and ψ_q, L_d and L_q represent stator voltages $\vec{u}_o$, stator currents $\vec{i}_o$, magnet flux and stator inductance in dq-coordinate, respectively; ψ_m represents the magnet flux linkage of PMSM; R_s is the resistance of stator; P_p is the number of pole pairs; J is the moment of inertia; ω_e and ω_m are the electrical and mechanical angular frequency of PMSM, respectively; m_l is the load moment and m_r is the frictional moment, which is proportional to the mechanic angular frequency with the friction coefficient k_r.

Proposed braking method with avoiding regenerative energy

In normal conditions, where the regenerative energy is allowed back to the grid. The chopper switch S_{B6} in the B6-clamp circuit is switched off. The system is protected by the B12-clamp circuit to avoid overvoltage. The DMC-fed PMSM drive operates in four-quadrant and the energy flows in both directions of DMC, which depends on the motor operation to be acceleration or braking.

In special cases, the regenerative energy back to the grid is not allowed, temporarily or completely. In practice, especially when the PMSM drive is fully loaded, the following features of the drive system are frequently desired:

- The regenerative energy could be fully avoided from feeding back to the grid.

- The braking torque of the motor drive is controllable and is able to keep relative constant without large fluctuation, so that the braking process is smooth and safe. Meanwhile, the braking torque should not exceed the required limitation.

To achieve this, in this proposed principle, the switching matrix of DMC will be shut down during braking, so that the regenerative energy produced by braking operation of the PMSM drives will be dissipated by the braking resistor R_{B6} in the B6-diode bridge, instead of flowing back to grid.

During braking process, the motor moment reference, which is the DC-link current $i_{B6,dc}$, will be controlled by setting the duty cycle V_t of the chopper switch S_{B6} based on the required moment limitation. The simplified circuit for analysing the braking process is shown in Fig. 3.

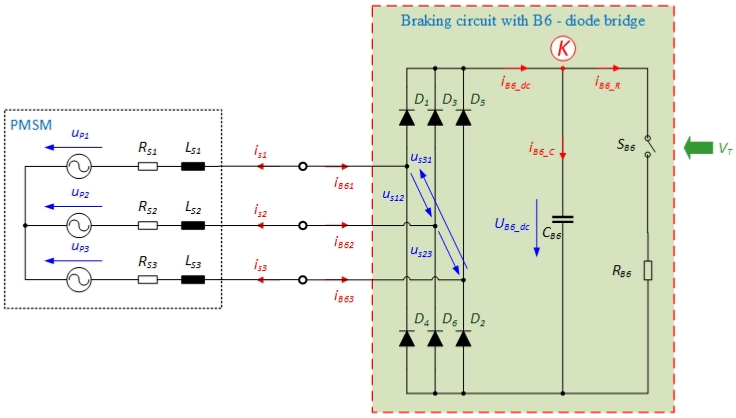

Fig. 3: Analyse of the braking circuit using B6-diode bridge for DMC-fed PMSM drives

It can be seen from Fig. 3 that the current of the chopper resistance $i_{B6,R}$ can be described in (11).

$$i_{B6,R} = \frac{U_{B6,dc}}{R_{B6}} \cdot V_t \quad , \quad (0 \leq V_t \leq 1) \tag{11}$$

where V_t is the duty cycle of chopper switch S_{B6}, which is limited between 0 and 1; R_{B6} is the chopper resistance.

If Kirchhoff's current law is employed in node K, then (12) can be obtained.

$$i_{B6,dc} = i_{B6,C} + i_{B6,R} = C_{B6} \cdot \frac{d(U_{B6,dc})}{dt} + \frac{U_{B6,dc}}{R_{B6}} \cdot V_t \quad , \quad (0 \leq V_t \leq 1) \tag{12}$$

Since the switching matrix is switched off during braking in this case and the three-phase motor currents are no longer represented by the three-phase output currents of DMC, in this strategy, the DC-link current in B6-diode bridge $i^*_{B6,dc}$ is employed in the outer current control loop as reference value to control the motor moment mi within the required limitation and without large fluctuation.

The output of the current control loop is used as reference voltage $U^*_{B6,dc}$ for the inner voltage control loop. In the voltage control loop, the capacitor voltage $U_{B6,dc}$ is controlled to drop smoothly, which is corresponding to the current motor speed. The output of the voltage control loop will be current of the chopper resistance $i_{B6,R}$, which is used to determine the duty cycle V_t of the chopper switch S_{B6} as can be derived from (11).

The block diagram of the closed cascade control loops is shown in Fig. 4.

The discrete-time integrator is employed in the control using Forward-Euler-Method. The expression for the approximation is shown in (13).

$$\frac{1}{s} = T_p \cdot \frac{z^{-1}}{1 - z^{-1}} \tag{13}$$

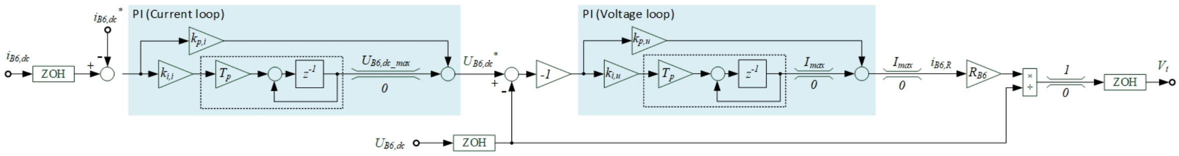

Fig. 4: Closed cascade control loops of the proposed braking method with avoiding regenerative energy

Simulation results

Simulation results in Fig. 5 is used to verify the feasibility of the proposed method using MATLAB. The parameters of the system are shown in Table I.

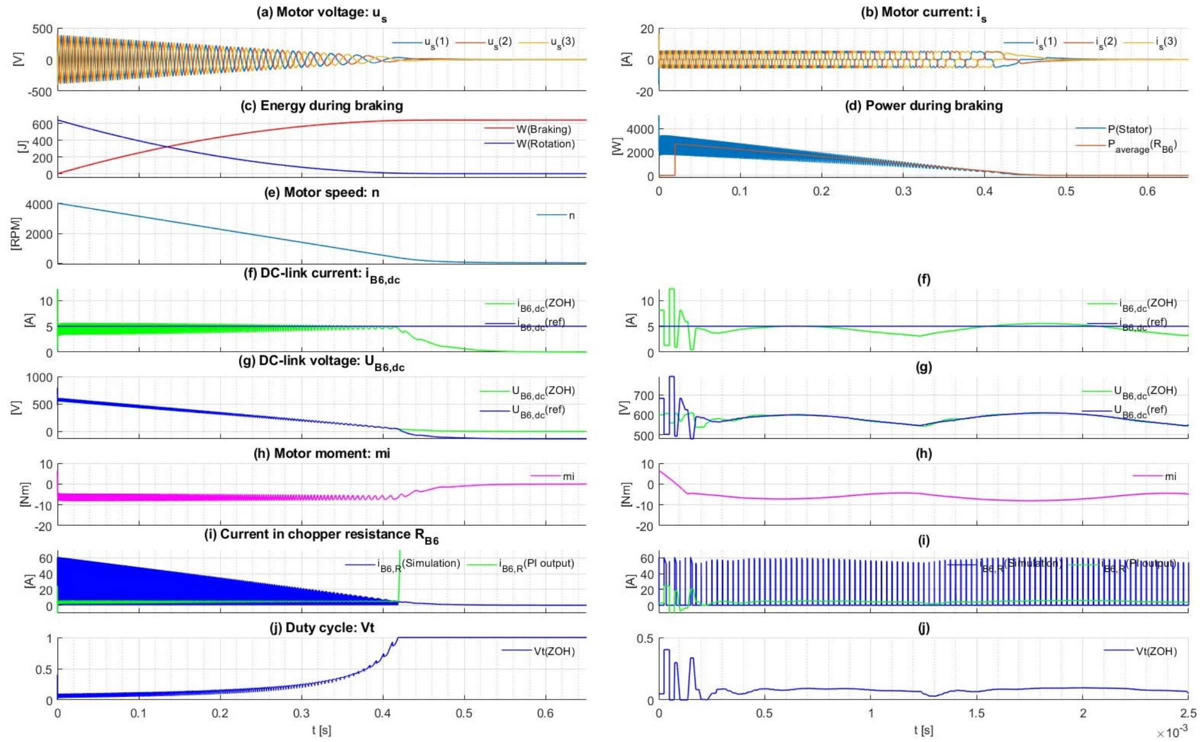

Fig. 5: Simulation results: (a) Motor voltage: $\vec{u}_s$. (b) Motor current: $\vec{i}_s$. (c) Energy during braking. (d) Power during braking. (d) Motor speed: n. (f) DC-link current: $i_{B6,dc}$. (g) DC-link voltage: $U_{B6,dc}$. (h) Motor moment: mi. (i) Current in chopper resistance R_{B6}. (j) Duty cycle V_t of chopper switch S_{B6}.

Table I: System parameter in simulation

Symbol	Value	Symbol	Value
C_{B6}	$5\mu F$	R_{B6}	10Ω
P_p	2	L_d, L_q	$4mH$
R_s	0.4Ω	J	$0.007 kg \cdot m^2$
ψ_m	$0.4V/(rad \cdot s^{-1})$	I_{max}	$70A$
f_p	$40kHz$		

In the simulation, the PMSM drive starts to brake by $t = 0$ from $4000RPM$ as shown in (e). The DC-link current $i^*_{B6,dc}$ in B6-diode bridge is set to be $5A$ as reference value for braking moment limitation and it can be well controlled through adjusting duty cycle V_t of the chopper switch S_{B6} as shown in (f) and (j). As the motor brakes, the motor speed decreases (g), as well as the motor voltage (a). This can also be indicated through the DC-link capacitor voltage $U_{B6,dc}$ as shown in (g).

The motor moment *mi* during braking is relative constant without large fluctuation as shown in (h), which shows a good result for braking moment limitation and also verifies the feasibility of the proposed control method.

Conclusion

In this paper, a simplified braking method with special consideration of avoiding regenerative energy is presented. By employing B6-diode bridge with one chopper resistance on motor side and shutting down the switching matrix of DMC during motor braking, the regenerative energy can be fully avoided from feeding back to the grid. Meanwhile, the braking torque is controlled within the required limitation and without large fluctuation, so that the braking process is smooth and safe. Simulation results confirm the feasibility of the proposed strategy.

References

[1] Alesina, A. and Venturini, M.: Solid-state power conversion: A Fourier analysis approach to generalized transformer synthesis, IEEE Transactions on Circuits and Systems, Vol 28 no 4, pp. 319-330, 1981.

[2] Alesina, A. and Venturini, M.G.B.: Analysis and design of optimum-amplitude nine-switch direct AC-AC converters, IEEE Transactions on Power Electronics, Vol 4 no 1, pp. 101-112, 1989.

[3] J. Rodriguez, M. Rivera, J.W. Kolar, P.W. Wheeler: A Review of Control and Modulation Methods for Matrix Converters, IEEE Transactions on Industrial Electronics, vol. 59, pp. 58-70, 2012.

[4] L. Empringham, J. W. Kolar, J. Rodriguez, P. W. Wheeler, J. C. Clare: Technological Issues and Industrial Application of Matrix Converters: A Review, IEEE Transactions on Industry Electronics, vol. 60, no. 10, pp. 4260-4271, Oct. 2013.

[5] J. Mahlein, J. Igney, J. Weigold, M. Braun, O. Simon: Matrix Converter Commutation Strategies With and Without Explicit Input Voltage Sign Measurement, IEEE Transactions on Industry Electronics, vol. 49, no. 2, pp. 407-414, April 2002.

[6] M. Imayavaramban, Patrick W. Wheeler, L. Empringham, Jon C. Clare: Input power clamp for controlling regeneration in matrix converter drive, IET, pp. 515-519, 2008.

[7] M. Imayavaramban, Patrick. W. Wheeler: Avoiding Regeneration with a Matrix Converter Drive, IEEE pp. 2529-2534, 2007.

[8] M. Imayavaramban, Patrick. W. Wheeler: Third method for regenerative braking in matrix converter drive: More electric aircraft, IEEE, pp. 1-6, 2017

[9] Tsuyoshi Nagano, Jun-ichi Itoh: Halt Sequence for Matrix Converter to Suppress Increase of Snubber Capacitor Voltage during Motor Regeneration, IEEE, pp. 6261-6266, 2016.

[10] She, Hongwu and Lin, Hua and Wang, Xingwei and Yue, Limin: Damped input filter design of matrix converter, PEDS, pp. 672-677, 2009.

[11] Costa, L. A. and Fan, B. and Burgos, R. and Boroyevich, D. and Chen, W. and Blasko, V.: The Fast Overvoltage Protection Consideration and Design for SiC-based Matrix Converters, APEC, pp. 1567-1574, 2020.

[12] Wheeler, P.W. and Rodriguez, J. and Clare, J.C. and Empringham, L. and Weinstein, A.: Matrix converters: a technology review, IEEE Transactions on Industrial Electronics, Vol 49 no 2, pp. 276-288, 2002.